MONOCLONAL ANTIBODIES IN IMMUNODIAGNOSIS AND IMMUNOTHERAPY
Volume 41, Number 2, 2022

DOI: 10.1089/mab.2021.0067

Development of a Monoclonal Antibody PMab-292 Against Ferret Podoplanin

Nohara Goto,[1] Hiroyuki Suzuki,[1] Tomohiro Tanaka,[2] Teizo Asano,[2] Mika K. Kaneko,[2] and Yukinari Kato[1,2]

Ferrets (*Mustela putorius furo*) have been used as small animal models to investigate severe acute respiratory syndrome coronaviruses (SARS-CoV and SARS-CoV-2) infections. Pathological analyses of these tissue samples, including those of the lung, are, therefore, essential to understand the pathogenesis of SARS-CoVs and evaluate the action of therapeutic monoclonal antibodies (mAbs) against this disease. However, mAbs that recognize ferret-derived proteins and distinguish between specific cell types, such as lung epithelial cells, are limited. Podoplanin (PDPN) has been identified as an essential marker in lung type I alveolar epithelial cells, kidney podocytes, and lymphatic endothelial cells. In this study, an anti-ferret PDPN (ferPDPN) mAb PMab-292 (mouse IgG_1, kappa) was established using the Cell-Based Immunization and Screening (CBIS) method. PMab-292 recognized ferPDPN-overexpressed Chinese hamster ovary-K1 (CHO/ferPDPN) cells by flow cytometry and Western blotting. The kinetic analysis using flow cytometry showed that the K_D of PMab-292 for CHO/ferPDPN was 3.4×10^{-8} M. Furthermore, PMab-292 detected lung type I alveolar epithelial cells, lymphatic endothelial cells, and glomerular/Bowman's capsule in the kidney using immunohistochemistry. Hence, these results propose the usefulness of PMab-292 in analyzing ferret-derived tissues for SARS-CoV-2 research.

Keywords: ferret podoplanin, monoclonal antibody, CBIS, immunohistochemistry

Introduction

Ferrets (*Mustela putorius furo*) have been used as a highly valuable model for testing the pathogenicity and transmission of human respiratory viruses, including the influenza virus,[1] severe acute respiratory syndrome coronavirus (SARS-CoV),[2] and SARS-CoV-2.[3] After mucosal exposure to SARS-CoV-2, clinical alterations in ferrets have been identified as undetectable or mild. In addition, they can transmit viruses efficiently to uninfected ferrets through direct contact and aerosols.[4,5] Similar to the golden (Syrian) hamster (*Mesocricetus auratus*) model, viral replication has also been detected in the upper respiratory tract of ferrets after a 2-week infection period. However, in contrast to the golden hamster,[6] reductions in body weight are absent or minimal.

In histopathological analysis, inflammation within alveolar spaces and perivascular mononuclear parts were observed in SARS-CoV-2-infected ferrets. In addition, the bronchial submucosal foci with eosinophilic materials and collagen degeneration were observed. Microscopic observations of SARS-CoV-2-infected ferrets, therefore, suggested mild bronchoalveolar or alveolar inflammation.[3] These studies also indicated that airborne transmission of SARS-CoV-2 can occur, thereby suggesting the usefulness of the ferret model in SARS-CoV-2 research.[7] However, there is a limitation of the pathological analysis owing to the lack of antibodies that can recognize the ferret-derived antigens and distinguish the specific cells in the lung.

Podoplanin (PDPN) is a type I transmembrane mucin-like sialoglycoprotein and an important marker in lung type I alveolar epithelial cells,[8,9] kidney podocytes,[10] and lymphatic endothelial cells.[11,12] Therefore, anti-ferret PDPN (ferPDPN) monoclonal antibodies (mAbs) have been proposed as a useful tool to investigate the pathogenesis of lung type I alveolar epithelial cells, kidney podocytes, and lymphatic endothelial cells in SARS-CoV-2 infection models. This study developed anti-ferPDPN mAbs using the Cell-

Departments of [1]Molecular Pharmacology and [2]Antibody Drug Development, Tohoku University Graduate School of Medicine, Sendai, Japan.

Based Immunization and Screening (CBIS) method. The CBIS method includes the immunization of antigen-overexpressed cells and subsequent high-throughput hybridoma screening through flow cytometry. We established an anti-ferPDPN mAb PMab-292 and investigated the several applications, including flow cytometry, Western blotting, and immunohistochemistry.

Materials and Methods

Cell lines

Chinese hamster ovary (CHO)-K1 and mouse multiple myeloma P3X63Ag8U.1 (P3U1) cells were obtained from the American Type Culture Collection (ATCC; Manassas, VA). Synthesized DNA (Eurofins Genomics KK, Tokyo, Japan) encoding ferPDPN plus an N-terminal MAP tag (GDGMVPPGIEDK)[13,14] and an N-terminal 2×RIEDL tag (RIEDLRIEDL),[15–20] which are recognized by an anti-MAP tag mAb (PMab-1) and an anti-RIEDL tag mAb (LpMab-7), respectively, were subcloned into a pCAG-Ble vector (FUJIFILM Wako Pure Chemical Corporation, Osaka, Japan). Afterward, plasmids were transfected into CHO-K1 cells, using Lipofectamine LTX with Plus Reagent (Thermo Fisher Scientific, Inc., Waltham, MA). Stable transfectants (CHO/MAP-ferPDPN and CHO/2×RIEDL-ferPDPN) were subsequently selected using cell sorter (SH800; Sony Corp., Tokyo, Japan).

Next, CHO-K1, CHO/MAP-ferPDPN, CHO/2×RIEDL-ferPDPN, and P3U1 were cultured in a Roswell Park Memorial Institute (RPMI) 1640 medium (Nacalai Tesque, Inc., Kyoto, Japan), supplemented with 10% heat-inactivated fetal bovine serum (Thermo Fisher Scientific, Inc.), 100 U/mL penicillin, 100 μg/mL streptomycin, and 0.25 μg/mL amphotericin B (Nacalai Tesque, Inc.). CHO/MAP-ferPDPN was cultivated in a medium containing 0.5 mg/mL Zeocin (InvivoGen, San Diego, CA). Cells were then cultured in an incubator at 37°C humidity, 5% CO_2, and 95% air atmosphere.

Hybridoma production

Female BALB/c mice (6-week-old) were purchased from CLEA, Japan (Tokyo, Japan). Animals were housed under specific pathogen-free conditions. The animal care and use committee of Tohoku University approved all animal experiments. In this study, we used a CBIS method[21–27] to develop mAbs against ferPDPN. One BALB/c mouse was subsequently immunized intraperitoneally (i.p.) with CHO/MAP-ferPDPN cells (1×10^8) using Imject Alum (Thermo Fisher Scientific, Inc.). The procedure included three additional immunization with CHO/MAP-ferPDPN cells (1×10^8), followed by a final booster injection of CHO/MAP-ferPDPN cells (1×10^8) 2 days before harvesting splenic cells.

Subsequently, splenic cells were fused with P3U1 cells using polyethylene glycol 1500 (PEG1500; Roche Diagnostics, Indianapolis, IN). The hybridomas were grown in RPMI 1640 media supplemented with hypoxanthine, aminopterin, and thymidine for selection (Thermo Fisher Scientific, Inc.), after which culture supernatants were screened through flow cytometry for anti-ferPDPN antibody production.

Flow cytometry

Cells (2×10^5 cells/mL) were harvested after brief exposure to 0.25% trypsin in 1 mM ethylenediaminetetraacetic acid (Nacalai Tesque, Inc.). After washing with 0.1% bovine serum albumin (Nacalai Tesque, Inc.) in phosphate-buffered saline (PBS; Nacalai Tesque, Inc.), cells were treated with PMab-292 (1–0.001 μg/mL) for 30 minutes at 4°C, followed by Alexa Fluor 488-conjugated anti-mouse IgG (1:1000; product no. 4408; Cell Signaling Technology, Inc., Danvers, MA). Finally, fluorescence data were collected using SA3800 Cell Analyzer (Sony Biotechnology Corp.).

Determining of the binding affinity

Cells were suspended in 100 μL serially diluted PMab-292 (10–0.0006 μg/mL), followed by a subsequent suspension in an Alexa Fluor 488-conjugated anti-mouse IgG solution (1:200; Cell Signaling Technology, Inc.). Afterward, fluorescence data were collected, using the BD FACSLyric (BD Biosciences, Franklin Lakes, NJ). By fitting binding isotherms to built-in one-site binding models in GraphPad Prism 8 (GraphPad Software, Inc., La Jolla, CA), the dissociation constant (K_D) was finally calculated.

Western blotting

Cell lysates (10 μg) were boiled in sodium dodecyl sulfate (SDS) sample buffer (Nacalai Tesque, Inc.), after which proteins were separated on 5%–20% polyacrylamide gels (FUJIFILM Wako Pure Chemical Corporation) and transferred to polyvinylidene difluoride membranes (Merck KGaA, Darmstadt, Germany). After blocking with 4% skim milk (Nacalai Tesque, Inc.) in 0.05% Tween 20-containing PBS, membranes were incubated with 1 μg/mL of PMab-292, an anti-MAP tag mAb (PMab-1), or an anti-β-actin mAb (clone AC-15; Sigma-Aldrich Corp., St. Louis, MO). Then, they were incubated again with peroxidase-conjugated anti-mouse immunoglobulins (diluted 1:1000; Agilent Technologies, Inc., Santa Clara, CA). Finally, protein bands were detected using ImmunoStar LD (FUJIFILM Wako Pure Chemical Corporation) and a Sayaca-Imager (DRC Co. Ltd., Tokyo, Japan).

Immunohistochemical analysis

Ferret tissue samples were collected after autopsy procedures were completed at the Yamaguchi University, and fixed in 10% neutral-buffered formalin,[28] after which paraffin-embedded tissue sections (4 μm thick) were made. Subsequently, histological sections (4 μm thick) of ferret tissue samples were directly autoclaved in a citrate buffer (pH 6.0; Nichirei Biosciences, Inc., Tokyo, Japan) for 20 minutes. After blocking histological sections with a SuperBlock T20 (PBS) Blocking Buffer (Thermo Fisher Scientific, Inc.), sections were incubated with PMab-292 (5 μg/mL) for 1 hour at room temperature and treated with the EnVision+Kit for mouse (Agilent Technologies, Inc.) for 30 minutes.

Color was developed with 3,3′-diaminobenzidine tetrahydrochloride (Agilent Technologies, Inc.) for 2 minutes, after counterstaining using hematoxylin (FUJIFILM Wako Pure Chemical Corporation). Hematoxylin and eosin (FUJIFILM Wako Pure Chemical Corporation) staining was also conducted using the serial section of ferret tissue samples.

Results

Establishment of anti-ferPDPN mAbs

To develop anti-ferPDPN mAbs, the CBIS method, using stable transfectants for immunization and flow cytometry, was used (Fig. 1). CHO/MAP-ferPDPN cells, which overexpressed ferPDPN and had an N-terminal MAP tag (also referred to as CHO/ferPDPN) were immunized into one mouse. Hybridomas were then seeded into 96-well plates, and CHO/2×RIEDL-ferPDPN-positive and CHO-K1-negative wells were identified. After conducting limiting dilution and selection using immunohistochemistry, the PMab-292 (mouse IgG_1, kappa) was finally isolated.

Flow cytometric analyses

Flow cytometric analyses were conducted using PMab-292 with CHO/ferPDPN and CHO-K1 cells. PMab-292 recognized CHO/ferPDPN, but did not react with CHO-K1 cells (Fig. 2A). The kinetic analysis of PMab-292 interactions with CHO/ferPDPN cells was, therefore, conducted using flow cytometry. As indicated in Figure 2B, the K_D for PMab-292 interactions with CHO/ferPDPN cells was 3.4×10^{-8} M, suggesting that PMab-292 exhibited a moderate affinity for ferPDPN.

Western blotting

Western blotting was conducted to further assess the sensitivity of PMab-292. For this assessment, lysates of CHO-K1 and CHO/ferPDPN cells were probed. As demonstrated in Figure 3, PMab-292 detected the 48-kDa band of ferPDPN in lysates from CHO/ferPDPN cells, whereas this band was absent in lysates from CHO-K1 cells, indicating that PMab-292 specifically detected ferPDPN.

Immunohistochemical analyses

To investigate whether PMab-292 can be used for immunohistochemical analyses using formalin-fixed paraffin-embedded (FFPE) ferret tissue sections, normal lung and kidney tissue samples from ferrets were examined. Both

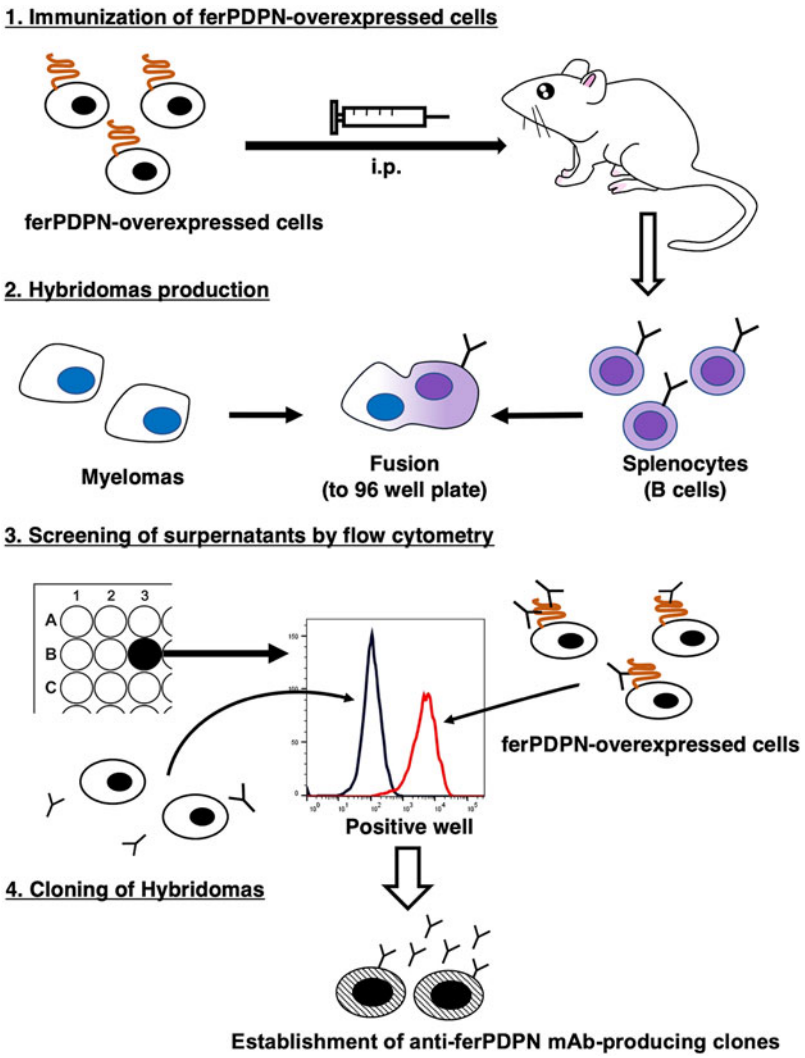

FIG. 1. Schematic procedure showing the CBIS method. CHO/ferPDPN cells were inoculated i.p. into the mice. Splenic cells were then fused with myeloma cells, after which culture supernatants from hybridomas were screened for anti-ferPDPN antibody production using flow cytometry. CBIS, Cell-Based Immunization and Screening; i.p., intraperitoneally.

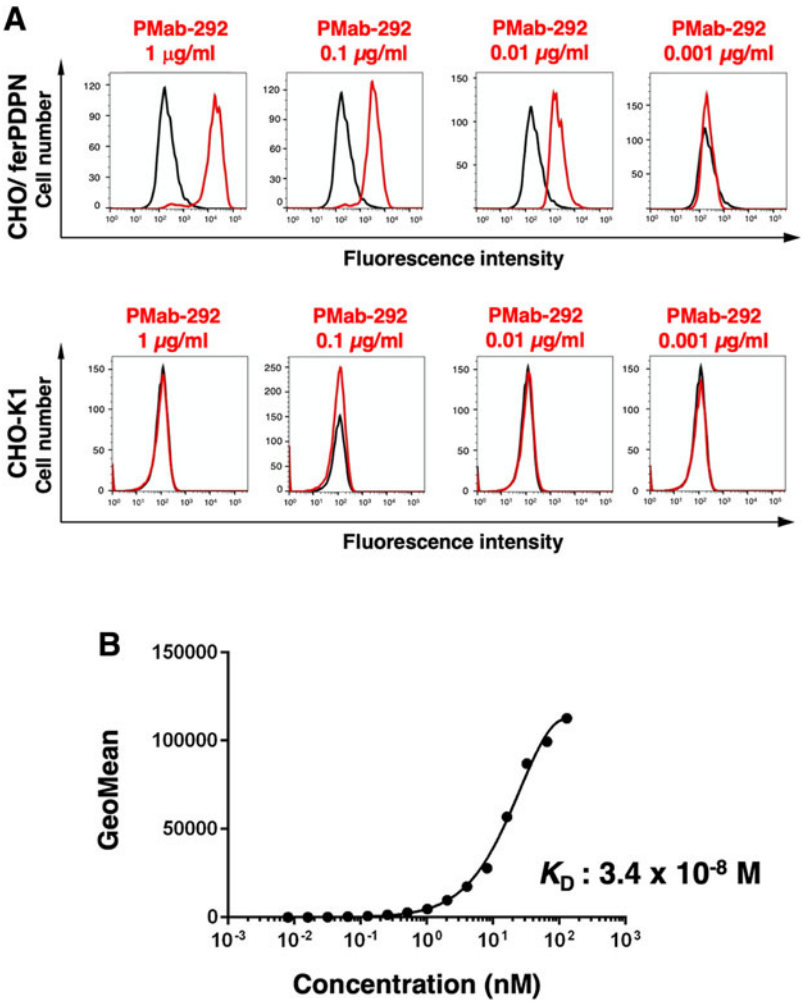

FIG. 2. Flow cytometry using anti-ferPDPN mAb, PMab-292. **(A)** CHO-K1 and CHO/ferPDPN were treated with 1–0.001 μg/mL of PMab-292, followed by treatment with Alexa Fluor 488-conjugated anti-mouse IgG. The black line represents the negative control. **(B)** CHO/ferPDPN cells were suspended in 100 μL serially diluted PMab-292 (10–0.0006 μg/mL), after subsequent treatment with Alexa Fluor 488-conjugated anti-mouse IgG. Fluorescence data were subsequently collected using BD FACSLyric, after which we calculated the dissociation constant (K_D) using GraphPad PRISM 8. mAb, monoclonal antibody.

tissue samples expressed PDPN in different species, including human,[29] mouse,[30] rat,[31] rabbit,[32] dog,[33] cat,[34] cow,[35] pig,[36] Tasmanian devil,[37] alpaca,[38] tiger,[39] whale,[40] goat,[41] horse,[42] bears,[43] and sheep.[24,44] As indicated in Figure 4, PMab-292 strongly and specifically identified type I alveolar cell within the lung. Lymphatic endothelial cells of the lung were also detected using PMab-292 (Fig. 4C). Moreover, PMab-292 was clearly stained in the glomerulus and Bowman's capsule in the kidney (Fig. 5A, B). Therefore, these results indicated the usefulness of PMab-292 for detecting ferPDPN-positive cells in FFPE tissue samples.

Discussion

Previously, we reported the cross-reactivity of anti-bear PDPN mAb (PMab-241) with ferret PDPN-overexpressed cells and ferret tissue samples.[28] Through flow cytometry, PMab-241 recognized ferret PDPN-overexpressed CKO-K1 cells. PMab-241 also reacted with lymphatic endothelial cells, but not with type I alveolar epithelial cells in the ferret lung. In this study, we established a novel anti-ferret PDPN mAb, PMab-292, which is useful for flow cytometry and immunohistochemical staining. Especially, PMab-292 stained type I alveolar epithelial cells of the ferret lung (Fig. 4). Therefore, PMab-292 can be used to detect and analyze the development and/or pathogenesis of type I alveolar epithelial cells. Previously, we have conducted a conventional alanine-scanning method[16,24,45–65] and the REMAP method[17–20] to determine conformational epitopes of mAbs. Further studies are also warranted to determine the epitope of PMab-292 using those methods.

Ferrets have been used as animal models for investigating the pathogenicity and transmission of both SARS-CoV and SARS-CoV-2. Therefore, we can compare the pathogenesis of viral-based respiratory tract infections. SARS-CoV infections demonstrated bronchial and bronchiolar hyperplasia, and perivascular cuffing in ferret lung tissue samples. However, no evidence of enhanced disease was observed in any ferret.[66] With SARS-CoV-2 infections in ferrets, several reports proposed that the clinical disease remained mild compared with the golden hamsters.[67]

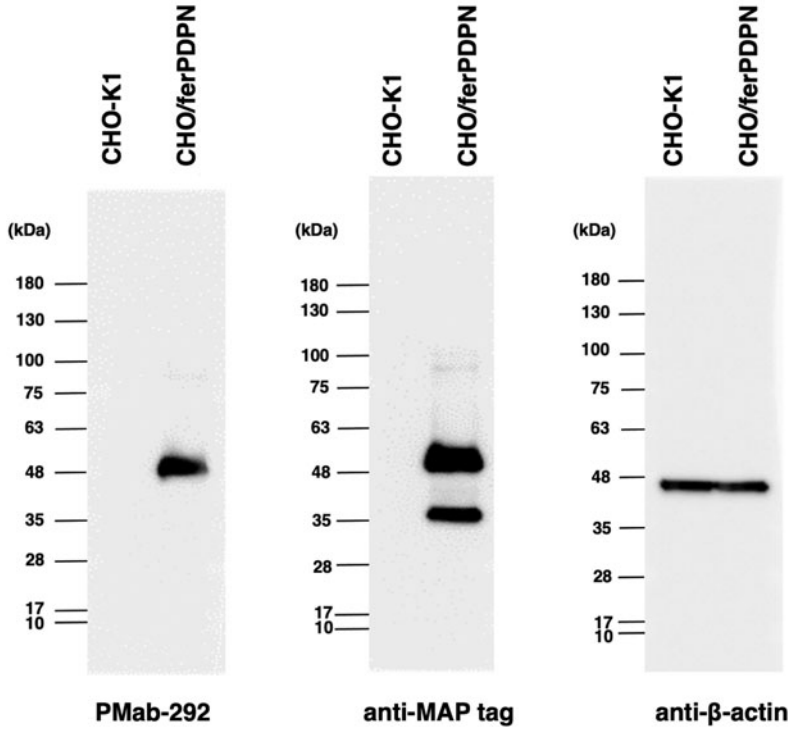

FIG. 3. Western blotting using PMab-292. Cell lysates (10 μg) of CHO-K1 and CHO/ferPDPN cells were electrophoresed, after which proteins were transferred to PVDF membranes. After blocking, membranes were subsequently incubated with 1 μg/mL PMab-292, anti-MAP tag mAb (PMab-1), and anti-β-actin, followed by incubation with peroxidase-conjugated anti-mouse immunoglobulins. PVDF, polyvinylidene difluoride.

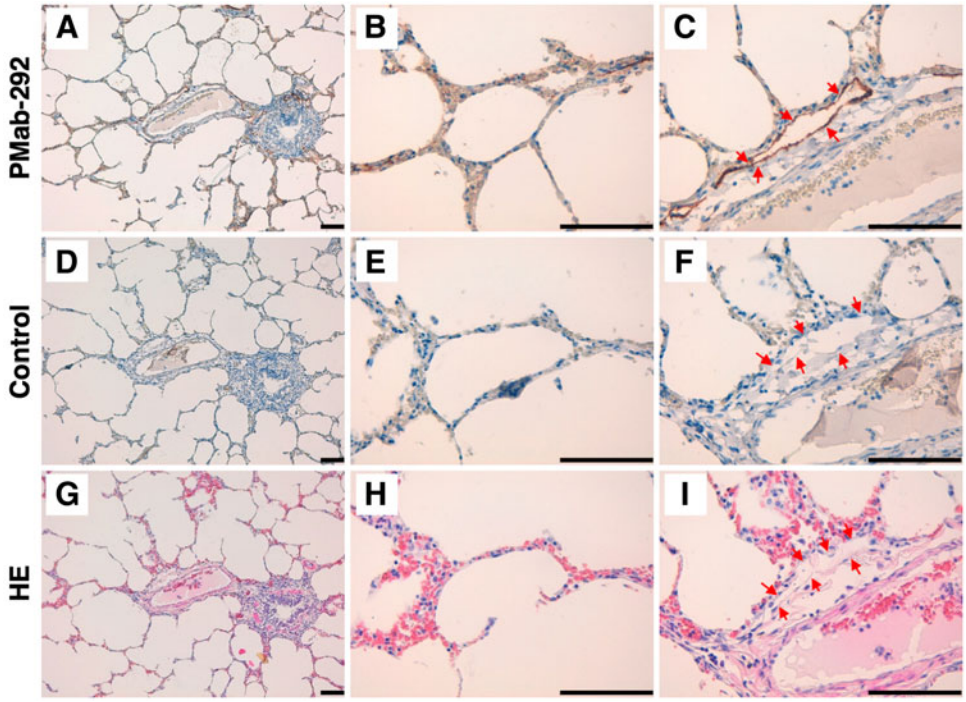

FIG. 4. Immunohistochemical analysis for the ferret lung. Histological sections of the ferret lung were directly autoclaved in a citrate buffer and incubated with 5 μg/mL of PMab-292 **(A–C)** or a blocking buffer **(D–F)**, followed by the EnVision+Kit. **(G–I)** H&E staining was performed. Arrows show that PDPN was expressed in lymphatic endothelial cells. Scale bars = 100 μm. H&E, hematoxylin and eosin.

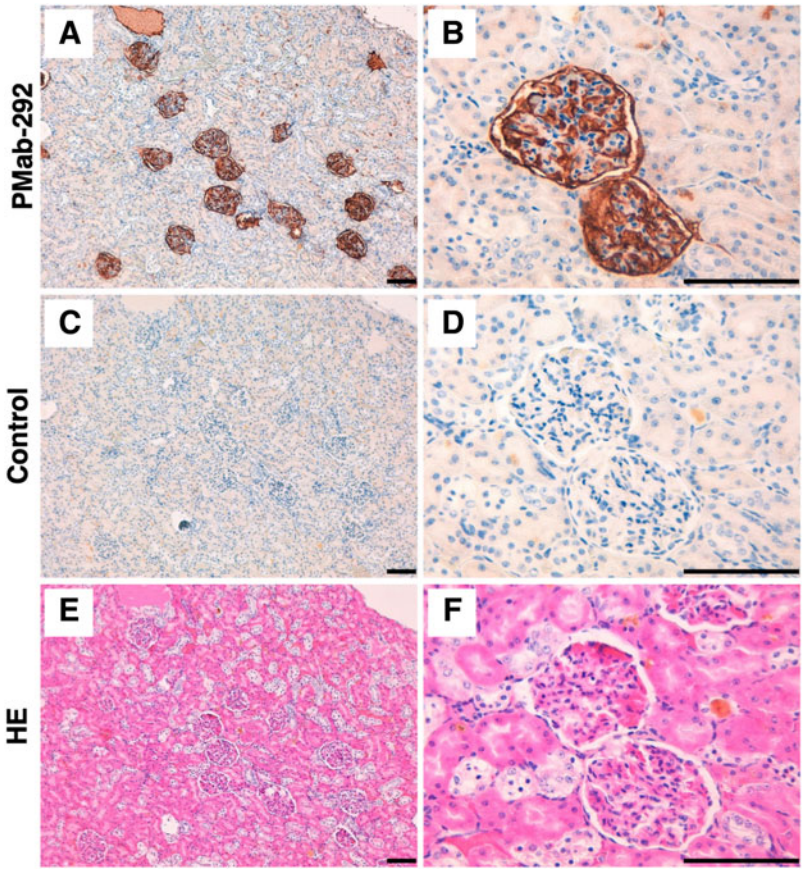

FIG. 5. Immunohistochemical analysis for the ferret kidney. Histological sections from the ferret kidney were directly autoclaved in a citrate buffer and incubated with 5 μg/mL of PMab-292 **(A, B)** or blocking buffer **(C, D)**, followed by the EnVision+Kit. **(E, F)** H&E staining. Scale bars = 100 μm.

Nevertheless, a persistent inflammation in the nasal turbinates was observed in young ferrets, after which follicular hyperplasia in the bronchi developed 21-day postinfection.[68] Therefore, the ferret model of SARS-CoV-2 infection resembles human asymptomatic infection.[69] The use of PMab-292 to investigate the morphological alterations in lung type I alveolar epithelial cells is also proposed to provide valuable information on the pathogenesis of viral infections, thereby contributing to the development of drugs against these infections, including the SARS-CoV-2.

Author Disclosure Statement

No competing financial interests exist.

Funding Information

This research was supported in part by Japan Agency for Medical Research and Development (AMED) under Grant Nos. JP21am0401013 and JP21am0101078 (to Y.K.).

References

1. Nguyen TQ, Rollon R, and Choi YK: Animal models for influenza research: Strengths and weaknesses. Viruses 2021;13:1011.
2. van den Brand JM, Haagmans BL, van Riel D, Osterhaus AD, and Kuiken T: The pathology and pathogenesis of experimental severe acute respiratory syndrome and influenza in animal models. J Comp Pathol 2014;151:83–112.
3. Muñoz-Fontela C, Dowling WE, Funnell SGP, Gsell PS, Riveros-Balta AX, Albrecht RA, Andersen H, Baric RS, Carroll MW, Cavaleri M, Qin C, Crozier I, Dallmeier K, de Waal L, de Wit E, Delang L, Dohm E, Duprex WP, Falzarano D, Finch CL, Frieman MB, Graham BS, Gralinski LE, Guilfoyle K, Haagmans BL, Hamilton GA, Hartman AL, Herfst S, Kaptein SJF, Klimstra WB, Knezevic I, Krause PR, Kuhn JH, Le Grand R, Lewis MG, Liu WC, Maisonnasse P, McElroy AK, Munster V, Oreshkova N, Rasmussen AL, Rocha-Pereira J, Rockx B, Rodríguez E, Rogers TF, Salguero FJ, Schotsaert M, Stittelaar KJ, Thibaut HJ, Tseng CT, Vergara-Alert J, Beer M, Brasel T, Chan JFW, García-Sastre A, Neyts J, Perlman S, Reed DS, Richt JA, Roy CJ, Segalés J, Vasan SS, Henao-Restrepo AM, and Barouch DH: Animal models for COVID-19. Nature 2020;586:509–515.
4. Kim YI, Kim SG, Kim SM, Kim EH, Park SJ, Yu KM, Chang JH, Kim EJ, Lee S, Casel MAB, Um J, Song MS, Jeong HW, Lai VD, Kim Y, Chin BS, Park JS, Chung KH, Foo SS, Poo H, Mo IP, Lee OJ, Webby RJ, Jung JU, and Choi YK: Infection and rapid transmission of SARS-CoV-2 in ferrets. Cell Host Microbe 2020;27:704–709.e702.
5. Shi J, Wen Z, Zhong G, Yang H, Wang C, Huang B, Liu R, He X, Shuai L, Sun Z, Zhao Y, Liu P, Liang L, Cui P, Wang J, Zhang X, Guan Y, Tan W, Wu G, Chen H, and

Bu Z: Susceptibility of ferrets, cats, dogs, and other domesticated animals to SARS-coronavirus 2. Science 2020; 368:1016–1020.
6. Sia SF, Yan LM, Chin AWH, Fung K, Choy KT, Wong AYL, Kaewpreedee P, Perera R, Poon LLM, Nicholls JM, Peiris M, and Yen HL: Pathogenesis and transmission of SARS-CoV-2 in golden hamsters. Nature 2020;583:834–838.
7. Richard M, Kok A, de Meulder D, Bestebroer TM, Lamers MM, Okba NMA, Fentener van Vlissingen M, Rockx B, Haagmans BL, Koopmans MPG, Fouchier RAM, and Herfst S: SARS-CoV-2 is transmitted via contact and via the air between ferrets. Nat Commun 2020;11:3496.
8. Dobbs LG, Williams MC, and Gonzalez R: Monoclonal antibodies specific to apical surfaces of rat alveolar type I cells bind to surfaces of cultured, but not freshly isolated, type II cells. Biochim Biophys Acta 1988;970:146–156.
9. Rishi AK, Joyce-Brady M, Fisher J, Dobbs LG, Floros J, VanderSpek J, Brody JS, and Williams MC: Cloning, characterization, and development expression of a rat lung alveolar type I cell gene in embryonic endodermal and neural derivatives. Dev Biol 1995;167:294–306.
10. Breiteneder-Geleff S, Matsui K, Soleiman A, Meraner P, Poczewski H, Kalt R, Schaffner G, and Kerjaschki D: Podoplanin, novel 43-kd membrane protein of glomerular epithelial cells, is down-regulated in puromycin nephrosis. Am J Pathol 1997;151:1141–1152.
11. Hirakawa S, Hong YK, Harvey N, Schacht V, Matsuda K, Libermann T, and Detmar M: Identification of vascular lineage-specific genes by transcriptional profiling of isolated blood vascular and lymphatic endothelial cells. Am J Pathol 2003;162:575–586.
12. Petrova TV, Mäkinen T, Mäkelä TP, Saarela J, Virtanen I, Ferrell RE, Finegold DN, Kerjaschki D, Ylä-Herttuala S, and Alitalo K: Lymphatic endothelial reprogramming of vascular endothelial cells by the Prox-1 homeobox transcription factor. EMBO J 2002;21:4593–4599.
13. Fujii Y, Kaneko MK, and Kato Y: MAP tag: A novel tagging system for protein purification and detection. Monoclon Antib Immunodiagn Immunother 2016;35:293–299.
14. Wakasa A, Kaneko MK, Kato Y, Takagi J, and Arimori T: Site-specific epitope insertion into recombinant proteins using the MAP tag system. J Biochem 2020;168:375–384.
15. Asano T, Kaneko MK, and Kato Y: RIEDL tag: A novel pentapeptide tagging system for transmembrane protein purification. Biochem Biophys Rep 2020;23:100780.
16. Sayama Y, Sano M, Kaneko MK, and Kato Y: Epitope analysis of an anti-whale podoplanin monoclonal antibody, PMab-237, using flow cytometry. Monoclon Antib Immunodiagn Immunother 2020;39:17–22.
17. Sano M, Kaneko MK, Aasano T, and Kato Y: Epitope mapping of an antihuman EGFR monoclonal antibody (EMab-134) using the REMAP method. Monoclon Antib Immunodiagn Immunother 2021;40:191–195.
18. Asano T, Kaneko MK, Takei J, Tateyama N, and Kato Y: Epitope mapping of the anti-CD44 monoclonal antibody (C44Mab-46) using the REMAP method. Monoclon Antib Immunodiagn Immunother 2021;40:156–161.
19. Asano T, Kaneko MK, and Kato Y: Development of a novel epitope mapping system: RIEDL insertion for epitope mapping method. Monoclon Antib Immunodiagn Immunother 2021;40:162–167.
20. Nanamiya R, Sano M, Asano T, Yanaka M, Nakamura T, Saito M, Tanaka T, Hosono H, Tateyama N, Kaneko MK, and Kato Y: Epitope mapping of an anti-human epidermal growth factor receptor monoclonal antibody (EMab-51) using the RIEDL insertion for epitope mapping method. Monoclon Antib Immunodiagn Immunother 2021;40:149–155.
21. Itai S, Fujii Y, Nakamura T, Chang YW, Yanaka M, Saidoh N, Handa S, Suzuki H, Harada H, Yamada S, Kaneko MK, and Kato Y: Establishment of CMab-43, a sensitive and specific anti-CD133 monoclonal antibody, for immunohistochemistry. Monoclon Antib Immunodiagn Immunother 2017;36:231–235.
22. Furusawa Y, Kaneko MK, and Kato Y: Establishment of an anti-CD20 monoclonal antibody (C(20)Mab-60) for immunohistochemical analyses. Monoclon Antib Immunodiagn Immunother 2020;39:112–116.
23. Furusawa Y, Kaneko MK, and Kato Y: Establishment of C(20)Mab-11, a novel anti-CD20 monoclonal antibody, for the detection of B cells. Oncol Lett 2020;20:1961–1967.
24. Kaneko MK, Sano M, Takei J, Asano T, Sayama Y, Hosono H, Kobayashi A, Konnai S, and Kato Y: Development and characterization of anti-sheep podoplanin monoclonal antibodies PMab-253 and PMab-260. Monoclon Antib Immunodiagn Immunother 2020;39:144–155.
25. Tanaka T, Asano T, Sano M, Takei J, Hosono H, Nanamiya R, Nakamura T, Yanaka M, Harada H, Fukui M, Suzuki H, Uchida K, Nakagawa T, Kato Y, and Kaneko MK: Development of monoclonal antibody PMab-269 against California Sea Lion podoplanin. Monoclon Antib Immunodiagn Immunother 2021;40:124–133.
26. Yamada S, Itai S, Nakamura T, Yanaka M, Chang YW, Suzuki H, Kaneko MK, and Kato Y: Monoclonal antibody L1Mab-13 detected human PD-L1 in lung cancers. Monoclon Antib Immunodiagn Immunother 2018;37:110–115.
27. Yamada S, Itai S, Nakamura T, Yanaka M, Kaneko MK, and Kato Y: Detection of high CD44 expression in oral cancers using the novel monoclonal antibody, C44Mab-5. Biochem Biophys Rep 2018;14:64–68.
28. Nanamiya R, Takei J, Asano T, Sano M, Tanaka T, Hosono H, Harada H, Sakai Y, Mizuno T, Suzuki H, Kaneko MK, and Kato Y: Ferret podoplanin is detected by PMab-241 in immunohistochemistry. Monoclon Antib Immunodiagn Immunother 2021;40:134–140.
29. Kato Y, Kaneko MK, Kuno A, Uchiyama N, Amano K, Chiba Y, Hasegawa Y, Hirabayashi J, Narimatsu H, Mishima K, and Osawa M: Inhibition of tumor cell-induced platelet aggregation using a novel anti-podoplanin antibody reacting with its platelet-aggregation-stimulating domain. Biochem Biophys Res Commun 2006;349:1301–1307.
30. Kaji C, Tsujimoto Y, Kato Kaneko M, Kato Y, and Sawa Y: Immunohistochemical examination of novel rat monoclonal antibodies against mouse and human podoplanin. Acta Histochem Cytochem 2012;45:227–237.
31. Oki H, Honma R, Ogasawara S, Fujii Y, Liu X, Takagi M, Kaneko MK, and Kato Y: Development of sensitive monoclonal antibody PMab-2 against rat podoplanin. Monoclon Antib Immunodiagn Immunother 2015;34:396–403.
32. Honma R, Fujii Y, Ogasawara S, Oki H, Liu X, Nakamura T, Kaneko MK, Takagi M, and Kato Y: Establishment of a novel monoclonal antibody PMab-32 against rabbit podoplanin. Monoclon Antib Immunodiagn Immunother 2016; 35:41–47.

33. Honma R, Kaneko MK, Ogasawara S, Fujii Y, Konnai S, Takagi M, and Kato Y: Specific detection of dog podoplanin expressed in renal glomerulus by a novel monoclonal antibody PMab-38 in immunohistochemistry. Monoclon Antib Immunodiagn Immunother 2016;35:212–216.
34. Yamada S, Itai S, Nakamura T, Yanaka M, Saidoh N, Chang YW, Handa S, Harada H, Kagawa Y, Ichii O, Konnai S, Kaneko MK, and Kato Y: PMab-52: specific and sensitive monoclonal antibody against cat podoplanin for immunohistochemistry. Monoclon Antib Immunodiagn Immunother 2017;36:224–230.
35. Honma R, Ogasawara S, Kaneko M, Fujii Y, Oki H, Nakamura T, Takagi M, Konnai S, and Kato Y: PMab-44 detects bovine podoplanin in immunohistochemistry. Monoclon Antib Immunodiagn Immunother 2016;35:186–190.
36. Kato Y, Yamada S, Furusawa Y, Itai S, Nakamura T, Yanaka M, Sano M, Harada H, Fukui M, and Kaneko MK: PMab-213: A monoclonal antibody for immunohistochemical analysis against pig podoplanin. Monoclon Antib Immunodiagn Immunother 2019;38:18–24.
37. Furusawa Y, Yamada S, Itai S, Nakamura T, Takei J, Sano M, Harada H, Fukui M, Kaneko MK, and Kato Y: Establishment of a monoclonal antibody PMab-233 for immunohistochemical analysis against Tasmanian devil podoplanin. Biochem Biophys Rep 2019;18:100631.
38. Kato Y, Furusawa Y, Yamada S, Itai S, Takei J, Sano M, and Kaneko MK: Establishment of a monoclonal antibody PMab-225 against alpaca podoplanin for immunohistochemical analyses. Biochem Biophys Rep 2019;18:100633.
39. Furusawa Y, Kaneko MK, Nakamura T, Itai S, Fukui M, Harada H, Yamada S, and Kato Y: Establishment of a monoclonal antibody PMab-231 for tiger podoplanin. Monoclon Antib Immunodiagn Immunother 2019;38:89–95.
40. Kato Y, Furusawa Y, Itai S, Takei J, Nakamura T, Sano M, Harada H, Yamada S, and Kaneko MK: Establishment of an anticetacean podoplanin monoclonal antibody PMab-237 for immunohistochemical analysis. Monoclon Antib Immunodiagn Immunother 2019;38:108–113.
41. Furusawa Y, Yamada S, Nakamura T, Sano M, Sayama Y, Itai S, Takei J, Harada H, Fukui M, Kaneko MK, and Kato Y: PMab-235: A monoclonal antibody for immunohistochemical analysis against goat podoplanin. Heliyon 2019;5:e02063.
42. Furusawa Y, Yamada S, Itai S, Sano M, Nakamura T, Yanaka M, Handa S, Mizuno T, Maeda K, Fukui M, Harada H, Kaneko MK, and Kato Y: Establishment of monoclonal antibody PMab-202 against horse podoplanin. Monoclon Antib Immunodiagn Immunother 2018;37:233–237.
43. Takei J, Furusawa Y, Yamada S, Nakamura T, Sayama Y, Sano M, Konnai S, Kobayashi A, Harada H, Kaneko MK, and Kato Y: PMab-247 detects bear podoplanin in immunohistochemical analysis. Monoclon Antib Immunodiagn Immunother 2019;38:171–174.
44. Kato Y, Furusawa Y, Sano M, Takei J, Nakamura T, Yanaka M, Okamoto S, Handa S, Komatsu Y, Asano T, Sayama Y, and Kaneko MK: Development of an anti-sheep podoplanin monoclonal antibody PMab-256 for immunohistochemical analysis of lymphatic endothelial cells. Monoclon Antib Immunodiagn Immunother 2020;39:82–90.
45. Chang YW, Kaneko MK, Yamada S, and Kato Y: Epitope mapping of monoclonal antibody PMab-52 against cat podoplanin. Monoclon Antib Immunodiagn Immunother 2018;37:95–99.
46. Chang YW, Yamada S, Kaneko MK, and Kato Y: Epitope mapping of monoclonal antibody PMab-38 against dog podoplanin. Monoclon Antib Immunodiagn Immunother 2017;36:291–295.
47. Furusawa Y, Yamada S, Itai S, Nakamura T, Fukui M, Harada H, Kaneko MK, and Kato Y: Elucidation of critical epitope of anti-rat podoplanin monoclonal antibody PMab-2. Monoclon Antib Immunodiagn Immunother 2018;37:188–193.
48. Honma R, Fujii Y, Ogasawara S, Oki H, Konnai S, Kagawa Y, Takagi M, Kaneko MK, and Kato Y: Critical epitope of anti-rabbit podoplanin monoclonal antibodies for immunohistochemical analysis. Monoclon Antib Immunodiagn Immunother 2016;35:65–72.
49. Kaneko MK, Furusawa Y, Sano M, Itai S, Takei J, Harada H, Fukui M, Yamada S, and Kato Y: Epitope mapping of the antihorse podoplanin monoclonal antibody PMab-202. Monoclon Antib Immunodiagn Immunother 2019;38:79–84.
50. Kaneko MK, Nakamura T, Kunita A, Fukayama M, Abe S, Nishioka Y, Yamada S, Yanaka M, Saidoh N, Yoshida K, Fujii Y, Ogasawara S, and Kato Y: ChLpMab-23: Cancer-specific human-mouse chimeric anti-podoplanin antibody exhibits antitumor activity via antibody-dependent cellular cytotoxicity. Monoclon Antib Immunodiagn Immunother 2017;36:104–112.
51. Kaneko MK, Oki H, Hozumi Y, Liu X, Ogasawara S, Takagi M, Goto K, and Kato Y: Monoclonal antibody LpMab-9 recognizes O-glycosylated N-terminus of human podoplanin. Monoclon Antib Immunodiagn Immunother 2015;34:310–317.
52. Kaneko MK, Yamada S, Itai S, Chang YW, Nakamura T, Yanaka M, and Kato Y: Elucidation of the critical epitope of an anti-EGFR monoclonal antibody EMab-134. Biochem Biophys Rep 2018;14:54–57.
53. Kato Y, Kunita A, Fukayama M, Abe S, Nishioka Y, Uchida H, Tahara H, Yamada S, Yanaka M, Nakamura T, Saidoh N, Yoshida K, Fujii Y, Honma R, Takagi M, Ogasawara S, Murata T, and Kaneko MK: Antiglycopeptide mouse monoclonal antibody LpMab-21 exerts antitumor activity against human podoplanin through antibody-dependent cellular cytotoxicity and complement-dependent cytotoxicity. Monoclon Antib Immunodiagn Immunother 2017;36:20–24.
54. Kato Y, Ogasawara S, Oki H, Goichberg P, Honma R, Fujii Y, and Kaneko MK: LpMab-12 established by CasMab technology specifically detects sialylated O-Glycan on Thr52 of platelet aggregation-stimulating domain of human podoplanin. PLoS One 2016;11:e0152912.
55. Kato Y, Sayama Y, Sano M, and Kaneko MK: Epitope analysis of an antihorse podoplanin monoclonal antibody PMab-219. Monoclon Antib Immunodiagn Immunother 2019;38:266–270.
56. Kato Y, Takei J, Furusawa Y, Sayama Y, Sano M, Konnai S, Kobayashi A, Harada H, Takahashi M, Suzuki H, Yamada S, and Kaneko MK: Epitope mapping of anti-bear podoplanin monoclonal antibody PMab-247. Monoclon Antib Immunodiagn Immunother 2019;38:230–233.
57. Sano M, Kaneko MK, and Kato Y: Epitope mapping of monoclonal antibody PMab-233 against Tasmanian devil podoplanin. Monoclon Antib Immunodiagn Immunother 2019;38:261–265.

58. Sayama Y, Sano M, Asano T, Furusawa Y, Takei J, Nakamura T, Yanaka M, Okamoto S, Handa S, Komatsu Y, Nakamura Y, Yanagawa M, Kaneko MK, and Kato Y: Epitope mapping of PMab-241, a lymphatic endothelial cell-specific anti-bear podoplanin monoclonal antibody. Monoclon Antib Immunodiagn Immunother 2020;39:77–81.
59. Sayama Y, Sano M, Furusawa Y, Kaneko MK, and Kato Y: Epitope mapping of PMab-225 an anti-alpaca podoplanin monoclonal antibody using flow cytometry. Monoclon Antib Immunodiagn Immunother 2019;38:255–260.
60. Takei J, Itai S, Furusawa Y, Yamada S, Nakamura T, Sano M, Harada H, Fukui M, Kaneko MK, and Kato Y: Epitope mapping of anti-tiger podoplanin monoclonal antibody PMab-231. Monoclon Antib Immunodiagn Immunother 2019;38:129–132.
61. Tanaka T, Asano T, Sano M, Takei J, Hosono H, Nanamiya R, Tateyama N, Kaneko MK, and Kato Y: Epitope mapping of the anti-California Sea Lion podoplanin monoclonal antibody PMab-269 using alanine-scanning mutagenesis and ELISA. Monoclon Antib Immunodiagn Immunother 2021;40:196–200.
62. Yamada S, Itai S, Furusawa Y, Kaneko MK, and Kato Y: Epitope mapping of antipig podoplanin monoclonal antibody PMab-213. Monoclon Antib Immunodiagn Immunother 2019;38:224–229.
63. Yamada S, Itai S, Kaneko MK, Konnai S, and Kato Y: Epitope mapping of anti-mouse podoplanin monoclonal antibody PMab-1. Biochem Biophys Rep 2018;15:52–56.
64. Yamada S, Kaneko MK, Itai S, Chang YW, Nakamura T, Yanaka M, Ogasawara S, Murata T, Uchida H, Tahara H, Harada H, and Kato Y: Epitope mapping of monoclonal antibody PMab-48 against dog podoplanin. Monoclon Antib Immunodiagn Immunother 2018;37:162–165.
65. Takei J, Asano T, Suzuki H, Kaneko MK, and Kato Y: Epitope mapping of the anti-CD44 monoclonal antibody (C44Mab-46) using alanine-scanning mutagenesis and surface plasmon resonance. Monoclon Antib Immunodiagn Immunother 2021;40:219–226.
66. Darnell ME, Plant EP, Watanabe H, Byrum R, St Claire M, Ward JM, and Taylor DR: Severe acute respiratory syndrome coronavirus infection in vaccinated ferrets. J Infect Dis 2007;196:1329–1338.
67. Monchatre-Leroy E, Lesellier S, Wasniewski M, Picard-Meyer E, Richomme C, Boué F, Lacôte S, Murri S, Pulido C, Vulin J, Salguero FJ, Gouilh MA, Servat A, and Marianneau P: Hamster and ferret experimental infection with intranasal low dose of a single strain of SARS-CoV-2. J Gen Virol 2021;102:001567.
68. van de Ven K, van Dijken H, Wijsman L, Gomersbach A, Schouten T, Kool J, Lenz S, Roholl P, Meijer A, van Kasteren PB, and de Jonge J: Pathology and immunity after SARS-CoV-2 infection in male ferrets is affected by age and inoculation route. Front Immunol 2021;12:750229.
69. Everett HE, Lean FZX, Byrne AMP, van Diemen PM, Rhodes S, James J, Mollett B, Coward VJ, Skinner P, Warren CJ, Bewley KR, Watson S, Hurley S, Ryan KA, Hall Y, Simmons H, Núñez A, Carroll MW, Brown IH, and Brookes SM: Intranasal infection of ferrets with SARS-CoV-2 as a model for asymptomatic human infection. Viruses 2021;13:113.

Address correspondence to:
Yukinari Kato
Department of Molecular Pharmacology
Tohoku University Graduate School of Medicine
2-1, Seiryo-machi, Aoba-ku
Sendai 980-8575
Miyagi
Japan

E-mail: yukinarikato@med.tohoku.ac.jp

Received: December 24, 2021
Accepted: January 25, 2022